

# Episodic memory loss is related to hippocampal-mediated $\beta$ -amyloid deposition in elderly subjects

E. C. Mormino,<sup>1</sup> J. T. Kluth,<sup>2</sup> C. M. Madison,<sup>1</sup> G. D. Rabinovici,<sup>1,2,3</sup> S. L. Baker,<sup>2</sup> B. L. Miller,<sup>3</sup> R. A. Koeppe,<sup>4</sup> C. A. Mathis,<sup>5</sup> M. W. Weiner,<sup>6</sup> W. J. Jagust<sup>1,2,3</sup> and the Alzheimer's Disease Neuroimaging Initiative\*

1 Helen Wills Neuroscience Institute, University of California, Berkeley, CA, USA

2 The Department of Molecular Imaging and Neuroscience, Lawrence Berkeley National Laboratory, Berkeley, CA, USA

3 Memory and Aging Center and Department of Neurology, University of California San Francisco, San Francisco, CA, USA

4 Division of Nuclear Medicine, Department of Radiology, University of Michigan, Ann Arbor, MI, USA

5 Department of Radiology, University of Pittsburgh, Pittsburgh, PA, USA

6 Center for Imaging of Neurodegenerative Diseases, Department of Veterans Affairs Medical Center, San Francisco, CA, USA

\*Data used in the preparation of this article were obtained in part from the Alzheimer's Disease Neuroimaging Initiative (ADNI) database ([www.loni.ucla.edu/ADNI](http://www.loni.ucla.edu/ADNI)). As such the investigators within the ADNI contributed to the design and implementation of ADNI and/or provided data but did not participate in analysis or writing of this report. ADNI investigators are listed at [www.loni.ucla.edu/ADNI/Collaboration/ADNI\\_Authorship\\_list.pdf](http://www.loni.ucla.edu/ADNI/Collaboration/ADNI_Authorship_list.pdf).

Correspondence to: William Jagust,  
132 Barker Hall, MC#3190,  
University of California, Berkeley,  
Berkeley, CA 94720  
E-mail: [jagust@berkeley.edu](mailto:jagust@berkeley.edu)

Although  $\beta$ -amyloid (A $\beta$ ) plaques are a primary diagnostic criterion for Alzheimer's disease, this pathology is commonly observed in the brains of non-demented older individuals. To explore the importance of this pathology in the absence of dementia, we compared levels of amyloid deposition (via 'Pittsburgh Compound-B' (PIB) positron emission tomography (PET) imaging) to hippocampus volume (HV) and episodic memory (EM) in three groups: (i) normal controls (NC) from the Berkeley Aging Cohort (BAC NC,  $n=20$ ); (ii) normal controls (NC) from the Alzheimer's disease neuroimaging initiative (ADNI NC,  $n=17$ ); and (iii) PIB+ mild cognitive impairment subjects from the ADNI (ADNI PIB+ MCI,  $n=39$ ). Age, gender and education were controlled for in each statistical model, and HV was adjusted for intracranial volume (aHV). In BAC NC, elevated PIB uptake was significantly associated with smaller aHV ( $P=0.0016$ ) and worse EM ( $P=0.0086$ ). Within ADNI NC, elevated PIB uptake was significantly associated with smaller aHV ( $P=0.047$ ) but not EM ( $P=0.60$ ); within ADNI PIB+ MCI, elevated PIB uptake was significantly associated with both smaller aHV ( $P=0.00070$ ) and worse EM ( $P=0.046$ ). To further understand these relationships, a recursive regression procedure was conducted within all ADNI NC and PIB+ MCI subjects ( $n=56$ ) to test the hypothesis that HV mediates the relationship between A $\beta$  and EM. Significant correlations were found between PIB index and EM ( $P=0.0044$ ), PIB index and aHV ( $P<0.0001$ ), as well as between aHV and EM ( $P<0.0001$ ). When both aHV and PIB were included in the same model to predict EM, aHV remained significant ( $P=0.0015$ ) whereas PIB index was no longer significantly associated with EM ( $P=0.50$ ). These results are consistent with a model in which A $\beta$  deposition, hippocampal atrophy, and EM occur sequentially in elderly subjects, with A $\beta$  deposition as the primary event in this cascade. This pattern suggests that declining EM in older individuals may be caused by A $\beta$ -induced hippocampus atrophy.

**Keywords:** Pittsburgh Compound-B; magnetic resonance imaging;  $\beta$ -amyloid; hippocampus; preclinical Alzheimer's disease

**Abbreviations:** A $\beta$  =  $\beta$ -amyloid; NC = normal controls; PIB = Pittsburgh compound-B; PET = positron emission tomography

## Introduction

Although converging evidence across many fields suggests that the  $\beta$ -amyloid (A $\beta$ ) protein is a central etiologic event in the pathogenesis of Alzheimer's disease (Hardy and Selkoe, 2002; Walsh and Selkoe, 2007) the role of this pathology in stages preceding Alzheimer's disease, especially normal aging, is poorly understood. Post-mortem studies have consistently observed A $\beta$  pathology in normal elderly subjects (Tomlinson *et al.*, 1968; Hulette *et al.*, 1998; Davis *et al.*, 1999; Price and Morris, 1999; Knopman *et al.*, 2003; Bennett *et al.*, 2006), and it has been suggested that the presence of this pathology reflects the earliest stage in the development of Alzheimer's disease. Proving this hypothesis has been difficult due to limitations inherent in post-mortem analysis. The recent development of [<sup>11</sup>C]PIB ('Pittsburgh Compound-B' (PIB)), a positron emission tomography (PET) radiotracer that binds to fibrillar A $\beta$  plaques, provides the unique opportunity to quantify this pathology antemortem, while simultaneously testing cognitive status. Studies employing PIB-PET imaging show high tracer uptake in Alzheimer's disease (Klunk *et al.*, 2004; Kempainen *et al.*, 2006; Rowe *et al.*, 2007) and elevated tracer uptake in a subset of normal individuals (Mintun *et al.*, 2006; Pike *et al.*, 2007; Rowe *et al.*, 2007; Aizenstein *et al.*, 2008; Fotenos *et al.*, 2008; Jack *et al.*, 2008b). These results are consistent with post-mortem studies, validating the application of PIB-PET imaging towards understanding the role of A $\beta$  deposition in non-demented people.

Post-mortem studies report A $\beta$  pathology in 25–45% of normal elderly individuals, depending on the age of the cohort and the pathological criteria employed (Tomlinson *et al.*, 1968; Hulette *et al.*, 1998; Davis *et al.*, 1999; Price and Morris, 1999; Knopman *et al.*, 2003; Bennett *et al.*, 2006). Recent PIB-PET studies have found that 10–30% of cognitively NC show elevated PIB uptake (Mintun *et al.*, 2006; Pike *et al.*, 2007; Rowe *et al.*, 2007; Fotenos *et al.*, 2008; Jack *et al.*, 2008b). These findings are consistent with the post-mortem frequencies after considering the younger cohort age in most PIB-PET studies. Although the general trend in post-mortem and PIB-PET studies has been to dichotomize NC into low- and high-A $\beta$  groups (referred to as 'PIB–' and 'PIB+' in PIB-PET studies), PIB uptake in published studies of normal older people clearly appears on a continuum, with PIB+ normal subjects usually showing lower levels than Alzheimer's disease patients (Pike *et al.*, 2007; Rowe *et al.*, 2007; Jack *et al.*, 2008b). This pattern supports the hypothesis that A $\beta$  accumulation is a continuous process that results in clinical Alzheimer's disease once a certain threshold is reached. Thus, examining A $\beta$  accumulation as a continuous variable, rather than dichotomizing subjects into PIB+ and PIB– groups, may yield further insights into the contribution of A $\beta$  to cognitive dysfunction in normal older individuals, emphasizing the need to examine early A $\beta$  accumulation as a continuous variable rather than dichotomizing into PIB+ and PIB– groups.

Episodic memory (EM) deficits are common in aging, particularly with respect to encoding new information (Small *et al.*, 1999).

Furthermore, EM decline has been associated with conversion to Alzheimer's disease (Small *et al.*, 2000; Grober *et al.*, 2008), and the relationship between the presence of A $\beta$  pathology in normal older people and EM needs to be further studied. Post-mortem studies examining the relationship between A $\beta$  pathology and EM have yielded inconsistent results, perhaps reflecting methodological limitations such as long delays between antemortem cognitive testing and autopsy (Katzman *et al.*, 1988; Hulette *et al.*, 1998; Schmitt *et al.*, 2000; Goldman *et al.*, 2001). Recent PIB-PET studies have examined this relationship, with one research group reporting an association between PIB uptake and EM (Pike *et al.*, 2007; Villemagne *et al.*, 2008).

Hippocampus volume (HV) atrophy has been shown to occur at a rate of 1.7% per year in individuals over age 60 (Raz and Rodrigue, 2006), and has also been associated with Alzheimer's disease (de Leon *et al.*, 1996; Jack *et al.*, 1999; Apostolova *et al.*, 2006; Smith *et al.*, 2007). It is unclear whether atrophy in this structure is related to A $\beta$  pathology in normal subjects. Jack *et al.* (2008b) found an association between PIB uptake and HV when non-demented subjects were combined with Alzheimer's disease subjects, as well as a non-significant trend for an association between elevated PIB and smaller HV within NC subjects.

We hypothesize that if A $\beta$  burden in non-demented populations represents the earliest signs of Alzheimer's disease, then this pathology should correlate with putative preclinical markers of Alzheimer's disease. Our study addresses this issue by comparing PIB uptake to HV and EM within normal elderly individuals. To determine whether observed relationships generalize to other populations, analyses were replicated in independent samples of NC and mild cognitive impairment subjects from the Alzheimer's disease Neuroimaging Initiative (ADNI, <http://www.adni-info.org/>).

## Methods

### Design overview

The relationships between A $\beta$  burden and preclinical Alzheimer's disease markers were examined in two independent groups of NC subjects. The primary analysis was performed in cognitively normal subjects from the Berkeley Aging Cohort (BAC NC), and a confirmatory analysis was performed in NC subjects from the Alzheimer's disease Neuroimaging Initiative (ADNI NC). Analyses were also conducted in ADNI mild cognitive impairment subjects showing elevated levels of PIB uptake (ADNI PIB+ MCI). Due to study protocol differences, data collection and processing between BAC and ADNI cohorts differ as discussed in detail below.

### Subject recruitment

BAC NC subjects were recruited from the community via newspaper advertisement. Eligibility requirements include age  $\geq$ 60, living independently in the community, normal performance on cognitive tests, absence of neurological or psychiatric illness and lack of major medical

illnesses and medications that affect cognition. One hundred nineteen subjects [mean age = 72.1(8.1), mean MMSE = 29.0(1.5)] are currently enrolled in the BAC. Twenty BAC subjects underwent PIB-PET imaging and magnetic resonance imaging (MRI) for this study. BAC subjects recruited for this study scored above 27 on the MMSE and below 10 on the Geriatric Depression Scale.

PIB-PET data for 20 Alzheimer's disease patients recruited from the University of California San Francisco (UCSF) Memory and Aging Center were used for comparison purposes. The diagnosis of Alzheimer's disease was based on a comprehensive multi-disciplinary evaluation that includes a clinical history and physical examination, a caregiver interview and a battery of neuropsychological tests (Kramer *et al.*, 2003). All Alzheimer's disease subjects meet NINDS criteria for probable Alzheimer's disease (McKhann *et al.*, 1984). No other significant co-morbid medical, neurologic or psychiatric illnesses were present.

The ADNI is a large multi-site collaborative effort launched in 2003 by the National Institute on Aging, the National Institute of Biomedical Imaging and Bioengineering, the Food and Drug Administration, private pharmaceutical companies and non-profit organizations as a public-private partnership aimed at testing whether serial MRI, PET, other biological markers and clinical and neuropsychological assessment can be combined to measure the progression of MCI and early AD. The Principal Investigator of this initiative is Michael Weiner, MD, and ADNI is the result of many co-investigators from a broad range of academic institutions and private corporations, with subjects recruited from over 50 sites across the US and Canada. ADNI NC subjects have MMSE scores between 24 and 30, have no memory complaints, have normal memory function as documented by performance on the Logical Memory II subscale (delayed paragraph recall) of the Wechsler Memory Scale-Revised (WMS-R) (Wechsler, 1987b), and a clinical dementia rating scale score of 0 (Morris, 1993). ADNI MCI subjects have MMSE scores between 24 and 30, have a memory complaint verified by an informant, documented abnormal memory function on the WMS-R paragraph recall, a CDR score of 0.5 and preservation of general cognition and function that excludes a diagnosis of Alzheimer's disease. Alzheimer's disease patients were required to meet published criteria for probable Alzheimer's disease with MMSE scores of 20–26 and CDR scores of 0.5 or 1. Further information on inclusion and exclusion criteria can be found at [www.adni-info.org](http://www.adni-info.org).

Subjects from the ADNI database were included in this study if they had completed PIB-PET imaging, structural MRI imaging, and cognitive testing. PIB uptake was compared to putative preclinical Alzheimer's disease markers in ADNI NC and MCI subjects meeting these criteria, whereas Alzheimer's disease subjects were used as a comparison group for PIB uptake. Three ADNI subjects meeting these criteria were excluded due to technical factors related to PET intensity normalization. Seventeen NC, 52 MCI, and 15 Alzheimer's disease subjects from ADNI were included in this study.

## Cognitive testing data

BAC subjects undergo a medical evaluation and detailed cognitive testing in multiple domains to assure normal functioning (episodic and working memory, language, visuospatial ability, frontal/executive ability). Cognitive composite scores across various domains were derived by averaging individual z-transformed test scores. Scores were z-transformed using mean and SDs from all BAC subjects 60 years and older. When applicable, z-transformed scores were inverted to make positive values correspond to better performance. Test scores within 6 months of PIB-PET imaging were used in statistical analyses.

If cognitive testing did not occur within 6 months of PIB-PET imaging, then an interpolated score was derived from testing sessions flanking the PET scanning session (interpolation was performed for five subjects, with a median duration between PET and closest cognitive testing date of 235 days).

EM composite scores were derived from the long delay free recall portion of the California verbal learning test (CVLT) (Delis, 2000) and WMS-R visual reproduction (Wechsler, 1987b). A working memory composite score was derived from the Wechsler adult intelligence scale (WAIS-R) digit span backwards (Wechsler, 1987a) and listening span total recall (Salthouse *et al.*, 1991). A frontal function composite score was derived from the Trails B minus A (Reitan, 1958) and Stroop total correct in 60 s (Zec, 1986).

ADNI participants undergo cognitive testing annually. Long delay free recall scores from the Rey Auditory Verbal Learning were used as a measure of EM. Mean and SDs from the ADNI NC PIB group were used to z-transform scores for all ADNI subjects (NC, MCI and Alzheimer's disease). ADNI subjects completed cognitive testing within 6 months of PIB-PET scanning (mean time and SD between cognitive testing and PET was  $36 \pm 40$  days).

## Radiotracer synthesis and PIB-PET acquisition

BAC NC and UCSF Alzheimer's disease subjects underwent PIB-PET scanning at the Lawrence Berkeley National Laboratory (LBNL). PIB was synthesized at this facility using a previously published protocol (Mathis *et al.*, 2003). In brief, high specific activity  $^{11}\text{C}$ -carbon dioxide produced on an 11 MeV CTI RDS-111 cyclotron was used to synthesize  $^{11}\text{C}$ - $\text{CH}_3$  (Langstrom *et al.*, 1987; Link *et al.*, 1997). The PIB precursor 2-(4'-aminophenyl)-6-methoxymethoxybenzothiazole was prepared and methylated with  $^{11}\text{C}$ - $\text{CH}_3$  prior to deprotection to afford the 6-hydroxy compound,  $^{11}\text{C}$ -PIB (Mathis *et al.*, 2003). The final compound was purified by semipreparative HPLC and injected at high specific activity. ADNI subjects underwent PIB scanning at 12 sites, using one of two methods to synthesize  $^{11}\text{C}$ -PIB: [ $^{11}\text{C}$ ]methyl iodide and a 6-MOM-protected precursor (Mathis *et al.*, 2003) or [ $^{11}\text{C}$ ]methyl triflate and an unprotected precursor (Wilson *et al.*, 2004). The minimum radiochemical purity was 90% and the minimum specific activity of the product at the time of injection was 300 Ci/mmol.

PIB-PET imaging for BAC and UCSF subjects was performed using a Siemens ECAT EXACT HR PET scanner in 3D acquisition mode. PIB (10–15 mCi) was injected into an antecubital vein. Dynamic acquisition frames were obtained as follows:  $4 \times 15$  s,  $8 \times 30$  s,  $9 \times 60$  s,  $2 \times 180$  s,  $8 \times 300$  s and  $3 \times 600$  s (90 min total). Ten minute transmission scans for attenuation correction were obtained for each PIB scan. PIB-PET data was reconstructed using an ordered subset expectation maximization algorithm with weighted attenuation. Images were smoothed with a 4 mm Gaussian kernel with scatter correction. ADNI PIB-PET images used in this study were collected at 12 different scanning sites. Dynamic acquisition frames were collected 50–70 min post-injection ( $4 \times 300$  s frames).

## MRI acquisition

Structural images for BAC NC subjects were collected at LBNL on a 1.5T Magnetom Avanto System (Siemens Inc., Iselin, NJ) with a 12 channel head coil run in triple mode. Three high-resolution structural T1-weighted volumetric magnetization prepared rapid gradient echo (MP-RAGE) scans were collected axially for each subject

(TR/TE/T1=2110/3.58/1100 ms, flip angle=15°, with 1.00 × 1.00 mm<sup>2</sup> in-plane resolution and 1.00 mm slice thickness). For 13 UCSF Alzheimer's disease subjects, MP-RAGE scans were collected coronally at UCSF on a 1.5T Vision System (Siemens Inc., Iselin, NJ) with a quadrature head coil (TR/TE/T1=10/7/300 ms, flip angle=15°, with 1.00 × 1.00 mm<sup>2</sup> in plane resolution and 1.40 mm slice thickness). For seven UCSF Alzheimer's disease subjects, MP-RAGE scans were collected sagittally on a Bruker MedSpec 4T system with an eight channel head coil (TR/TE/T1=2300/3.37/950 ms, flip angle=7°, with 1.00 × 1.00 mm<sup>2</sup> in-plane resolution and 1.00 mm slice thickness).

ADNI MRI scans are collected at multiple sites using either a GE, Siemens, or Philips 1.5T system. Two high-resolution T1-weighted volumetric MP-RAGE scans were collected for each subject. Parameter values vary depending on scanning site and can be found at <http://www.loni.ucla.edu/ADNI/Research/Cores/>. For this study, we used MP-RAGE scans that had undergone gradient warping correction (raw scans were used for images collected on Philips scanners, since these images do not require gradient warping correction) (Jack *et al.*, 2008a).

## PIB-PET processing

For BAC NC and UCSF Alzheimer's disease subjects, PIB-PET data was preprocessed using the SPM2 software package (<http://www.fil.ion.ucl.ac.uk/spm>). Realigned PIB frames corresponding to the first 20 min of acquisition were averaged and used to guide coregistration between each subject's PIB distribution volume ratio (DVR) image and structural MRI scan. A grey matter masked cerebellum reference region for PIB data was derived using the subject's averaged MP-RAGE scan via automated labeling (see section below). DVRs for PIB images were created using Logan graphical analysis with frames corresponding to 35–90 min post-injection (Logan *et al.*, 1996; Price *et al.*, 2005).

DVR images underwent partial volume correction to minimize signal washout in voxels adjacent to cerebrospinal fluid (Meltzer *et al.*, 1999; Zaidi *et al.*, 2006). Our partial volume correction procedure convolves a grey/white matter brain matter mask with a scanner-specific point-spread function. The resulting 3D image is used to correct radiotracer counts in the native space PET image by elevating voxels contaminated by cerebrospinal fluid.

In addition to creating partial volume corrected DVR images for BAC NC and UCSF Alzheimer's disease PIB data, these data were also analyzed using a standardized uptake value ratio (SUVR) approach (realigned frames corresponding to 50–70 min post-injection were averaged and normalized to mean value in cerebellum grey matter). SUVR images were not corrected for partial volume effects and were used to compare PIB values from our cohorts to PIB values derived from ADNI.

For ADNI subjects, all scans were checked for quality (counts, field-of-view, subject movement) and then SUVR images were created using the following processing steps: 50–70 min post-injection frames were realigned and averaged, processed to a standard orientation, image and voxel size, smoothed to a common resolution of 8 mm FWHM and intensity normalized to the mean uptake in cerebellum grey matter. Further information about image processing is available at [www.adni-info.org](http://www.adni-info.org). These preprocessing steps were completed by the ADNI PET core and were downloaded for use in this study. Partial volume correction was not applied to these data.

## ROI analysis

For all subjects, region of interest (ROI) labeling was implemented using the FreeSurfer software packages ([\[harvard.edu/\]\(http://surfer.nmr.mgh.harvard.edu/\)\). For BAC NC, three structural T1 scans for each subject were realigned and averaged to yield a single high-resolution image with excellent grey–white contrast. For UCSF AD, a single structural T1 image was processed through FreeSurfer. Structural images were bias field corrected, intensity normalized, and skull stripped using a watershed algorithm \(Dale \*et al.\*, 1999; Segonne \*et al.\*, 2004\). Manual touchup was performed to exclude all non-brain tissue \(resulting in a cleaned mask containing all grey/white matter and cerebrospinal fluid\). These images underwent a white matter-based segmentation, grey/white matter and pial surfaces were defined, and topology correction was applied to these reconstructed surfaces \(Dale \*et al.\*, 1999; Fischl \*et al.\*, 2001; Segonne \*et al.\*, 2004\). A trained operator \(ECM\) visually confirmed resulting surface output and made additional manual edits when necessary. Subcortical and cortical ROIs spanning the entire brain were defined in each subject's native space \(Fischl \*et al.\*, 2002; Desikan \*et al.\*, 2006\). Hippocampus and caudate ROIs from this step provided volumes for these structures \(averaged across the hemispheres\) and were used in subsequent regression models. The resulting cerebellum ROI \(grey matter only\) was used as a reference region to create PIB-DVR and SUVR images for BAC NC and UCSF Alzheimer's disease subjects. Additionally, multiple cortical ROIs were collapsed to yield four large ROIs that spanned prefrontal cortex \(all cortex anterior to the precentral sulcus\), lateral temporal cortex \(middle and superior temporal gyri\), parietal cortex \(supramarginal gyrus, inferior/superior parietal lobules and precuneus\), and anterior/posterior cingulate gyrus. A PIB index was the primary variable of interest in this study, and was derived by averaging the mean DVR value from these four ROIs. A PIB index from SUVR images was also extracted for BAC NC and Alzheimer's disease UCSF for comparison with ADNI PIB index values.](http://surfer.nmr.mgh.</a></p></div><div data-bbox=)

Grey and white matter components from the cleaned mask were combined and used to partial volume correct BAC and UCSF PIB-DVR images, and total volume of the cleaned mask (grey/white matter and cerebrospinal fluid) were used to adjust brain volumes by total intracranial volume (ICV).

MP-RAGE scans for ADNI subjects were processed through FreeSurfer as described above, although only two MP-RAGE scans for ADNI subjects were averaged. In addition, for ADNI cases an estimate of total ICV was derived using an automated atlas scaling method (Buckner *et al.*, 2004), and was used to adjust brain volumes. A PIB index was extracted for all ADNI subjects using SUVR images.

## Statistical models

All analyses were completed using the statistical programming language R, version 2.3 (<http://www.r-project.org/>). Welch two sample *t*-tests were used for group comparisons of continuous variables (age, education, MMSE and PIB index). Chi-squared tests were used to compare gender across groups.

A covariance approach was used to adjust HV by total ICV (Mathalon *et al.*, 1993). Adjusted HV (aHV) was obtained with the following formula:  $aHV = raw\ HV - b (ICV - mean\ ICV)$ , with *b* reflecting the regression coefficient when raw HV is regressed against ICV and mean ICV reflects the group mean. Regression coefficients and mean ICV for volume adjustments were calculated separately for each group analysis. Caudate and brain volume (grey/white matter combined) were corrected for ICV using the same covariance approach. Adjusted volumes were used in subsequent regression models.

Hierarchical multiple regression models were used to determine whether PIB index was significantly associated with putative preclinical Alzheimer's disease markers, controlling for the effects of age, gender and education. Two models were examined separately within BAC NC,

ADNI NC and ADNI PIB+ MCI groups: the first model used aHV as the dependent variable and the second model used EM as the dependent variable. Age, gender and education were entered into each model in the first step and PIB index was entered into each model in the second step. For each model, we report change in  $R^2$  ( $\Delta R^2$ ) to reflect the increase in  $R^2$  before and after PIB index is entered into the model. Partial regression plots were used to visualize the relationships between PIB index and aHV/EM (which displays the residuals of each variable after adjusting for age, gender and education). Using the same hierarchical regression approach, the relationship between aHV and EM was also examined within each group. Furthermore, 'control' hierarchical multiple regression models were executed within BAC NC, using caudate volume, brain volume, frontal function and working memory as dependent variables.

To test whether evidence exists for a sequential relationship between PIB index, aHV and EM, we implemented a recursive linear regression procedure used previously in a post-mortem study (Baron and Kenny, 1986; Bennett et al., 2004). Specifically, we hypothesized that hippocampus atrophy mediates the relationship between A $\beta$  burden and EM deficits in non-demented subjects. ADNI NC and PIB+ MCI were combined in this analysis ( $n=56$ ). In the first step of this approach, PIB index versus EM, PIB index versus aHV, and aHV versus EM are examined in separate regression models. In the second step, a multivariate model with PIB index and aHV simultaneously predicting EM was examined. Assuming the relationships in the first step are significant, the purposed sequential relationship is supported if aHV significantly predicts EM after controlling for PIB index (and PIB index does not significantly predict EM after controlling for aHV). Age, gender and education are controlled for in each model using the same hierarchical multiple regression approach described above. For this analysis, overall model  $R^2$  values are reported, as well as the  $\Delta R^2$  associated with PIB index and aHV during the multivariate step.

## Results

### BAC NC and UCSF Alzheimer's disease characteristics

Demographics and group PIB index values for BAC NC and UCSF Alzheimer's disease are summarized in Table 1. BAC NC and UCSF Alzheimer's disease did not significantly differ in education or gender. The UCSF Alzheimer's disease group was younger ( $t=-3.36$ ,  $P=0.0018$ ) and scored lower on the MMSE ( $t=-6.02$ ,

$P=0.0000102$ ) than the BAC NC group. Qualitative examination of cortical PIB uptake revealed a varied pattern across BAC NC and UCSF Alzheimer's disease subjects. Illustrative data from three individual subjects with Alzheimer's disease are shown in Fig. 1A–C, and are contrasted with three BAC NC subjects (Fig. 1D–F). In Alzheimer's disease subjects, high DVR values were typically found throughout cortical association areas, with relative sparing of primary cortical areas (i.e. motor/sensory cortex and occipital lobe, Fig. 1A–C). A number of subjects showed a more focal pattern, with elevated DVR in medial frontal cortex and precuneus/posterior cingulate (Fig. 1C). The BAC NC with the highest PIB uptake showed a pattern similar to a typical Alzheimer's disease case, with elevated uptake in the medial frontal cortex, precuneus, cingulate, and lateral temporo-parietal cortex (Fig. 1D). The BAC NC with the second highest PIB uptake showed localized deposition in medial frontal cortex and lateral parietal cortex (Fig. 1E). There were also NC subjects that did not have any indication of elevated DVR values throughout cortex (Fig. 1F). DVR PIB index values were significantly higher in UCSF Alzheimer's disease than BAC NC ( $t=8.49$ ,  $P=0.00000033$ , Fig. 2).

### Relationships between PIB index and preclinical Alzheimer's disease markers in BAC NC

Age, education and gender were not significantly associated with either aHV or EM in the BAC NC group. PIB index was significantly correlated with aHV ( $\Delta R^2=0.45$ ,  $t=-3.84$ ,  $P=0.0016$ ) and EM ( $\Delta R^2=0.35$ ,  $t=-3.02$ ,  $P=0.0086$ , Fig. 4). Furthermore, aHV was significantly associated with EM ( $\Delta R^2=0.27$ ,  $t=2.44$ ,  $P=0.028$ ). To examine the extent to which these relationships were influenced by subjects with elevated A $\beta$  burden, the two highest PIB index subjects (Fig. 1D–E) were removed from each regression model. In this subset analysis ( $n=18$ ), the PIB index versus aHV relationship remained significant ( $\Delta R^2=0.28$ ,  $t=-2.50$ ,  $P=0.026$ ), whereas significant relationships were no longer present in PIB index versus EM ( $\Delta R^2=0.03$ ,  $t=-0.74$ ,  $P=0.47$ ; Fig. 5) and aHV versus EM ( $\Delta R^2=0.11$ ,  $t=1.42$ ,  $P=0.18$ ).

**Table 1** Group Characteristics

	BAC NC	UCSF AD	ADNI NC	ADNI PIB– MCI	ADNI PIB+ MCI	ADNI AD
N	20	20	17	13	39	15
Age	72.3 (6.0)	64.3 (8.8)**	78.5 (5.4)	72.7 (7.8)*	75.0 (7.9)	72.6 (8.7)*
Gender	13F, 7M	9F, 11M	7F, 10M	3F, 10M	13F, 26M	5F, 10M
Education	18.3 (2.8)	16.7 (3.1)	14.9 (3.2)	16.8 (2.6)	16.2 (2.9)	14.9 (2.7)
MMSE	29.6 (0.6)	19.7 (6.7)***	28.6 (1.5)	27.1 (2.8)	27.4 (2.0)*	22.7 (2.9)***
PIB Index	SUVR: 1.40 (0.09); DVR: 1.44 (0.10)	SUVR: 2.02 (0.41)***; DVR: 2.13 (0.33)***	SUVR: 1.64 (0.49)	SUVR: 1.30 (0.10)*	SUVR: 2.14 (0.44)**	SUVR: 2.18 (0.45)**
Episodic Memory	–0.05 (0.85)	NA <sup>a</sup>	0.00 (1.0)	–1.29 (0.79)***	–1.11 (1.14)***	–1.89 (0.29)***

a Episodic memory scores were assessed with the CVLT 9 item variant in UCSF AD. Values are listed as mean (SD). In statistical contrasts, UCSF AD are compared to BAC NC; for ADNI groups, MCI and AD are compared to NC (\* $P<0.05$ , \*\* $P<0.01$ , \*\*\* $P<0.001$ ). For BAC NC and UCSF AD, PIB index values were computed using both DVR and SUVR approaches (DVR values were used for regression analyses, whereas SUVR values were used for comparison with ADNI values).

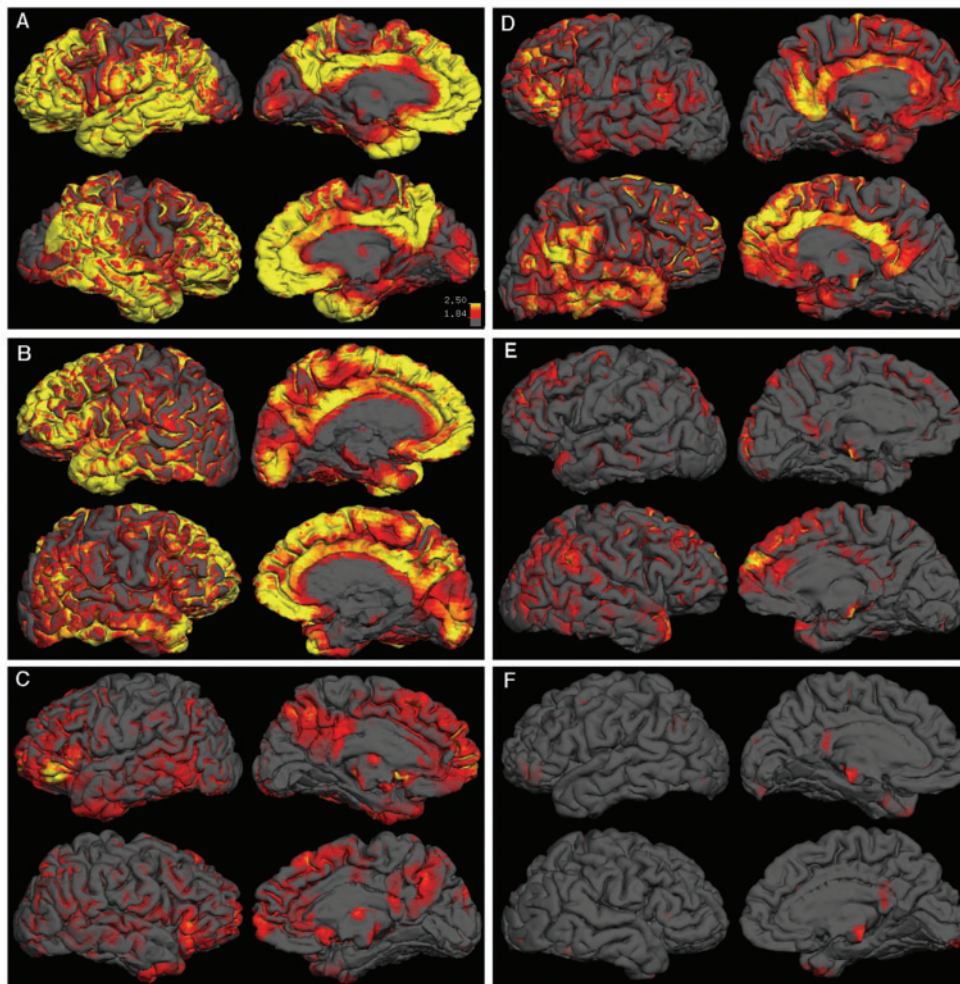


**Figure 1** Qualitative examination of PIB-DVR data. Partial volume corrected PIB-DVR images were overlaid on native space reconstructed surfaces derived from the subject's T1-weighted structural scan for 3 UCSF Alzheimer's disease subjects (A–C) and 3 BAC NC subjects (D–F). Each box shows lateral and medial views of PIB distribution for a single subject (left hemisphere is above right hemisphere in each box). All images reflect the same color scale, with yellow indicating high PIB uptake, red indicating medium PIB uptake, and grey indicating low PIB uptake.

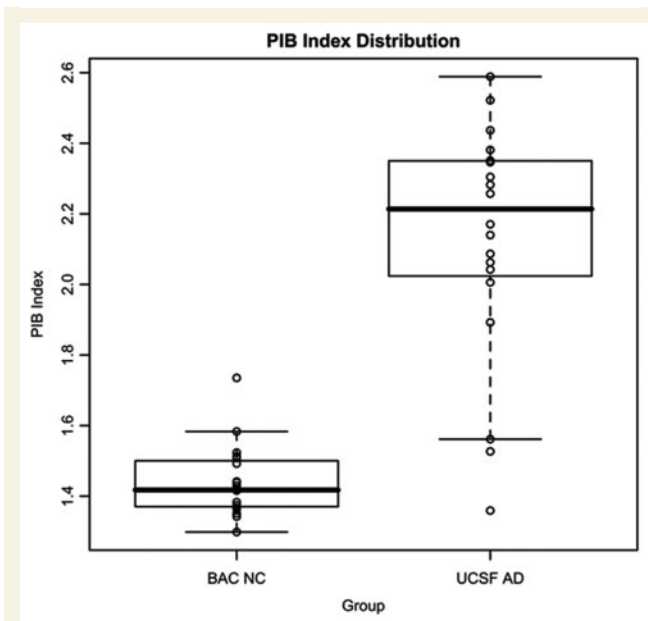
Within the BAC NC group, PIB index was not significantly correlated with caudate volume ( $\Delta R^2=0.0005$ ,  $t=0.094$ ,  $P=0.93$ ), whole brain volume ( $\Delta R^2=0.008$ ,  $t=0.41$ ,  $P=0.69$ ), working memory ( $\Delta R^2=0.15$ ,  $t=-1.55$ ,  $P=0.15$ ) or frontal function ( $\Delta R^2=0.06$ ,  $t=-0.97$ ,  $P=0.35$ ).

## ADNI group characteristics

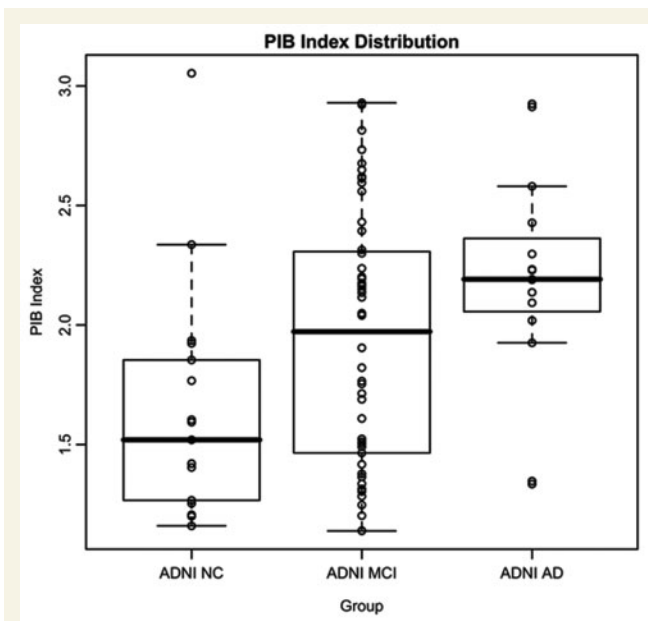
Demographics and group PIB index values for ADNI groups are summarized in Table 1. ADNI NC subjects did not significantly differ from Alzheimer's disease or MCI subjects in education or gender. NC subjects were significantly older than MCI ( $t=2.41$ ,  $P=0.021$ ) and Alzheimer's disease subjects ( $t=2.26$ ,  $P=0.034$ ). NC subjects scored significantly higher on the MMSE than MCI ( $t=2.86$ ,  $P=0.0066$ ) and Alzheimer's disease subjects ( $t=7.11$ ,  $P=6.81e-07$ ). NC subjects had higher EM scores than MCI ( $t=4.07$ ,  $P=0.00034$ ) and Alzheimer's disease ( $t=7.41$ ,  $P=5.03e-07$ ).

Figure 3 shows the distribution of SUVR PIB index values across the ADNI groups. Although the majority of Alzheimer's disease cases (13/15) show highly elevated PIB index values, NC and MCI subjects show a continuous range of values. Quantitatively, PIB index was significantly lower in NC compared to MCI ( $t=-2.09$ ,  $P=0.046$ ) and Alzheimer's disease ( $t=-3.30$ ,  $P=0.0025$ ). Additionally, there was a trend for MCI subjects to have lower PIB index than Alzheimer's disease subjects ( $t=-1.8773$ ,  $P=0.072$ ). It should be noted that the SUVR PIB index values in Fig. 3 are not directly comparable to the partial volume corrected DVR PIB index values displayed in Fig. 2. Direct comparison of SUVR and DVR PIB index values within the BAC NC group revealed an average difference of 5.5% between these two methods.

Interestingly, many demographic differences were present between BAC NC and ADNI NC groups. In comparison to ADNI NC, BAC NC were significantly younger ( $t=-3.29$ ,  $P=0.0023$ ), more educated ( $t=3.38$ ,  $P=0.0019$ ), and scored higher on the MMSE ( $t=2.52$ ,  $P=0.020$ ). There was no significant difference in gender between BAC and ADNI NC groups.



**Figure 2** Box and whiskers plot showing the distribution of DVR PIB index values in BAC NC and UCSF Alzheimer's disease subjects.



**Figure 3** Box and whiskers plot showing the distribution of SUVR PIB index values in ADNI groups. ADNI SUVR PIB index values are not directly comparable to BAC NC and UCSF Alzheimer's disease DVR PIB index values in Fig. 2 due to differences in image processing (see text).

## Relationships between PIB index and preclinical Alzheimer's disease markers in ADNI NC

Age, education and gender were not significantly associated with either aHV or EM within ADNI NC. PIB Index was significantly

associated with aHV ( $\Delta R^2=0.22$ ,  $t=-2.21$ ,  $P=0.047$ ), but was not significantly associated with EM ( $\Delta R^2=0.02$ ,  $t=0.53$ ,  $P=0.60$ ; Fig. 6). aHV was not significantly associated with EM in this group ( $\Delta R^2=0.01$ ,  $t=-0.44$ ,  $P=0.67$ ).

## Relationships between PIB index and preclinical Alzheimer's disease markers in ADNI PIB+ MCI

In order to assess whether similar relationships between these variables exist in subjects who are not demented but do have memory impairment, we utilized MCI subjects from the ADNI database as described above. For these subjects, we confined our analyses to cases that were defined as PIB+ (based on a threshold obtained via a receiver-operating characteristic (ROC) approach) in order to exclude MCI cases with hippocampus abnormalities that might be unrelated to Alzheimer's disease pathology, such as hippocampal sclerosis (Jicha *et al.*, 2006). SUVR PIB index values for BAC NC and UCSF Alzheimer's disease were used in this ROC curve analysis, and the resulting cut off was applied to ADNI MCI subjects.

A cut off value of 1.465 optimized discrimination between BAC NC and UCSF Alzheimer's disease subjects (sensitivity of 0.90 and specificity of 0.90 for the diagnosis of Alzheimer's disease) and was selected as the threshold for PIB-positivity. Application of this cut off value to the ADNI MCI cohort stratified 39/52 (75%) MCI subjects as PIB+ and 13/52 (25%) as PIB-. PIB+ MCI subjects were not significantly different from PIB- MCI subjects in age, gender, education, MMSE, aHV or EM ( $P>0.05$ ). Comparisons between ADNI NC and dichotomized MCI groups are summarized in Table 1. PIB- MCI subjects were not significantly different than NC subjects in gender, education or MMSE. PIB- MCI subjects were younger ( $t=-2.308$ ,  $P=0.032$ ), had lower PIB index values ( $t=-2.81$ ,  $P=0.012$ ) and lower EM scores ( $t=-3.96$ ,  $P=0.00047$ ) than NC subjects. PIB+ MCI subjects were not significantly different than NC in age, gender, or education. PIB+ MCI subjects scored lower on the MMSE ( $t=-2.64$ ,  $P=0.012$ ), had higher PIB index values ( $t=3.64$ ,  $P=0.0011$ ) and lower EM scores ( $t=-3.65$ ,  $P=0.00086$ ) than NC subjects.

Demographic variables were not significantly associated with either aHV or EM within the PIB+ MCI group. PIB index was significantly associated with aHV ( $\Delta R^2=0.27$ ,  $t=-3.73$ ,  $P=0.00070$ ) and EM ( $\Delta R^2=0.11$ ,  $t=-2.08$ ,  $P=0.046$ ; Fig. 7). Additionally, aHV was significantly associated with EM ( $\Delta R^2=0.28$ ,  $t=3.797$ ,  $P=0.00058$ ).

## Testing the sequential relationship between A $\beta$ pathology, hippocampus atrophy, and EM

ADNI NC and ADNI PIB+ MCI subjects were combined to test the hypothesized sequential relationship between the three variables of interest ( $n=56$ ). In the first step of this analysis, all three separate linear regression models were significant: PIB index predicting EM (overall model:  $R^2=0.17$ ,  $P=0.049$ ; PIB index:  $t=-2.983$ ,

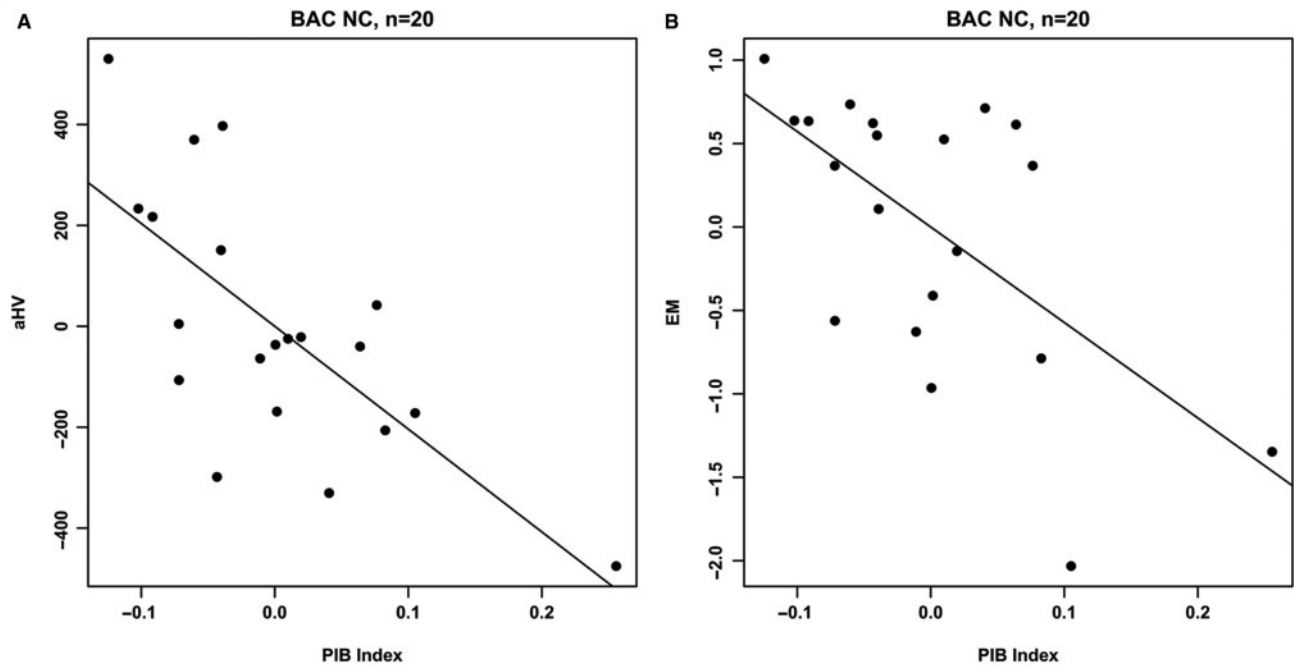


**Figure 4** Partial regression plots showing the relationships between PIB index and aHV (A) and EM (B) within the BAC NC group. Residuals are plotted for each variable to adjust for the effects of age; gender and education. Both regression models are significant (A:  $\Delta R^2 = 0.45$ ;  $P = 0.0016$ ; B:  $\Delta R^2 = 0.35$ ;  $P = 0.0086$ ).

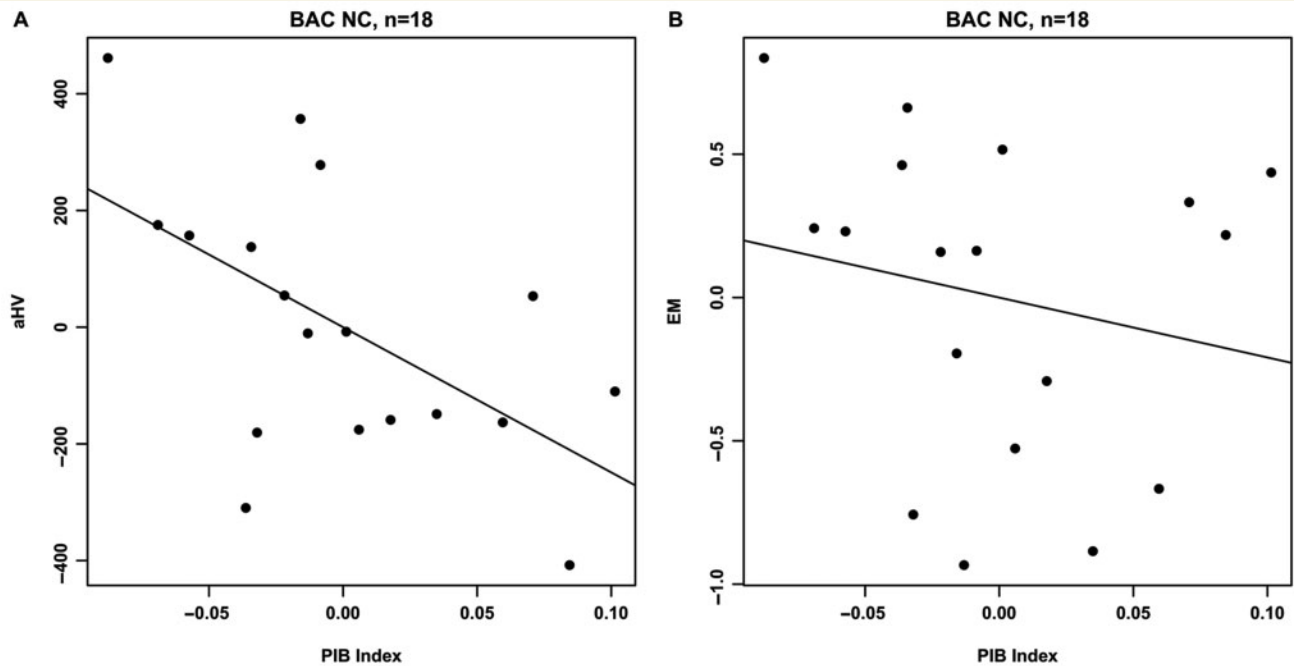


**Figure 5** Partial regression plots showing the relationships between PIB index and aHV (A) and EM (B) after removing the two subjects with the highest PIB uptake from the BAC NC group. Residuals are plotted for each variable to adjust for the effects of age, gender and education. PIB index versus aHV remains significant ( $\Delta R^2 = 0.28$ ,  $P = 0.026$ ), whereas PIB index versus EM is no longer significant ( $\Delta R^2 = 0.03$ ,  $P = 0.47$ ).

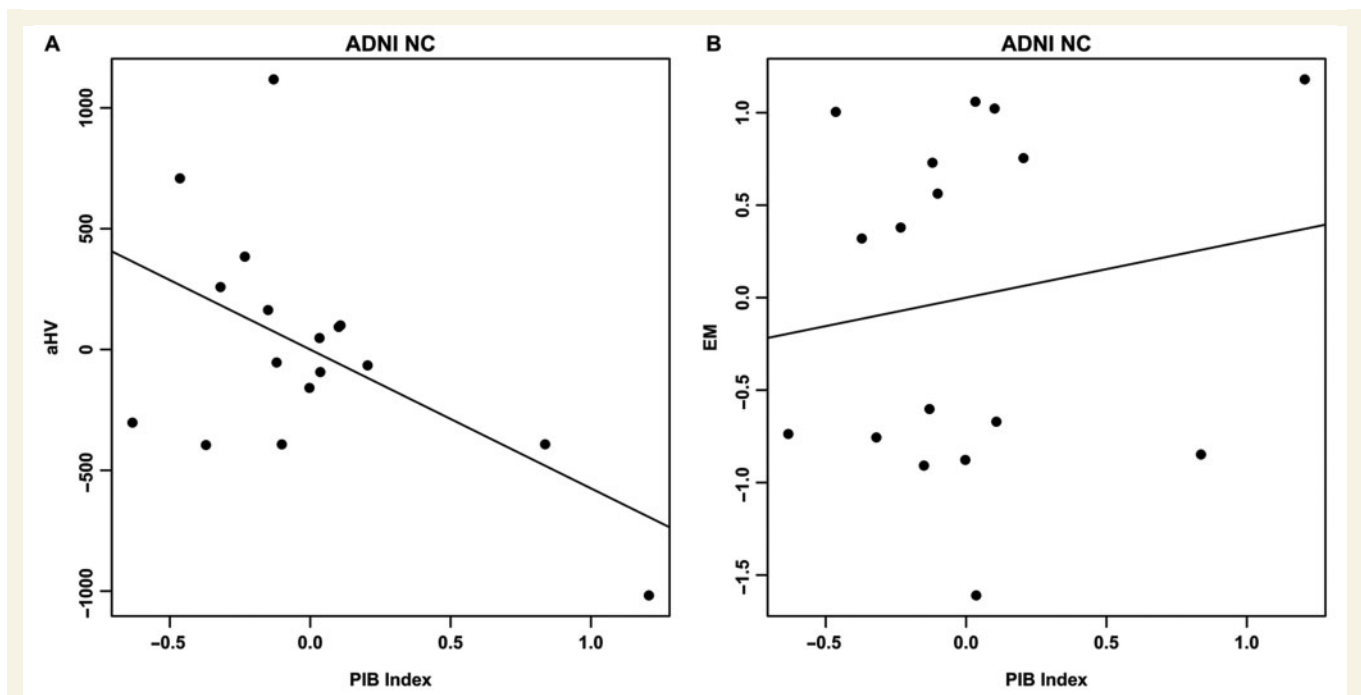


**Figure 6** Partial regression plots showing the relationships between PIB index and aHV (A) and EM (B) within the ADNI NC group. Residuals are plotted for each variable to adjust for the effects of age, gender and education. Only PIB index versus aHV shows a significant association (A:  $\Delta R^2=0.22$ ,  $P=0.047$ ; B:  $\Delta R^2=0.02$ ,  $P=0.60$ ).

$P=0.0044$ ), PIB index predicting aHV (overall model:  $R^2=0.38$ ,  $P=0.000061$ ; PIB index:  $t=-5.18$ ,  $P=0.0000038$ ), and aHV predicting EM (overall model:  $R^2=0.32$ ,  $P=0.00059$ ; aHV:  $t=4.662$ ,  $P=0.000023$ ). In the second step of this analysis, the model incorporating PIB index and aHV as simultaneous predictors of EM was also significant ( $R^2=0.32$ ,  $P=0.0013$ ). When examining the independent contributions of each predictor in this multivariate model, aHV remained significant ( $\Delta R^2=0.15$ ,  $t=3.36$ ,  $P=0.0015$ ) whereas PIB index was no longer significant ( $\Delta R^2=0.00$ ,  $t=-0.676$ ,  $P=0.50$ ; Fig. 8). These results are consistent with a model in which PIB index, aHV and EM are sequentially related, with aHV mediating the relationship between PIB index and EM.

## Discussion

In this study, we examined the relationships between A $\beta$  burden and putative preclinical Alzheimer's disease markers in multiple groups of non-demented subjects. Despite numerous differences across the examined cohorts, we consistently observed that higher PIB uptake was associated with reduced HV. Although PIB was associated with EM in our primary BAC NC group and the ADNI PIB+ MCI group, this relationship in BAC NC was driven by the two subjects with the highest PIB uptake and was not replicated in the ADNI NC group (Table 2). Furthermore, results from a recursive regression procedure support the hypothesis that HV mediates the relationship between PIB and EM. Overall, these results suggest that A $\beta$  and HV atrophy are directly related, whereas the relationship between A $\beta$  and EM is indirect and may be mediated by HV atrophy.

## A $\beta$ burden and Hippocampus Atrophy

The relationship between A $\beta$  burden and HV in the primary group of NC persisted after removal of the two subjects with the greatest PIB uptake, and was replicated in independent samples of NC and MCI subjects. Furthermore, PIB uptake was not correlated with the other brain volumes examined (caudate and whole brain volume), suggesting that the relationship between PIB uptake and HV is regionally specific and not due to general brain atrophy. This finding in normal subjects with relatively low PIB values implies that even slightly elevated global A $\beta$  levels may inflict damage or coincide with neurotoxic events in hippocampus. Although A $\beta$  plaques are not common in the medial temporal lobe (Arnold *et al.*, 1991), possible mechanisms exist that may explain the observed relationship between A $\beta$  burden and HV atrophy.

One possibility is that cortical A $\beta$  burden leads to HV atrophy by disrupting cortico-hippocampal connectivity. Cortical connections with the hippocampus are associated with successful memory formation (Ranganath *et al.*, 2005) and are compromised in Alzheimer's disease (Greicius *et al.*, 2004; Wang *et al.*, 2006). Thus, cortical plaques may disrupt cortico-hippocampal networks, resulting in HV atrophy as innervation to this structure is eliminated. Another explanation is that cortical deposition of A $\beta$  coincides with accumulation of neurofibrillary tangles (NFTs) in the hippocampus during the early stages of Alzheimer's disease development. Although post-mortem studies have shown that hippocampus atrophy correlates with NFTs (Braak and Braak, 1997; Jack *et al.*, 2002), hippocampus atrophy is an indirect measure of this pathology, and PET imaging agents that directly target

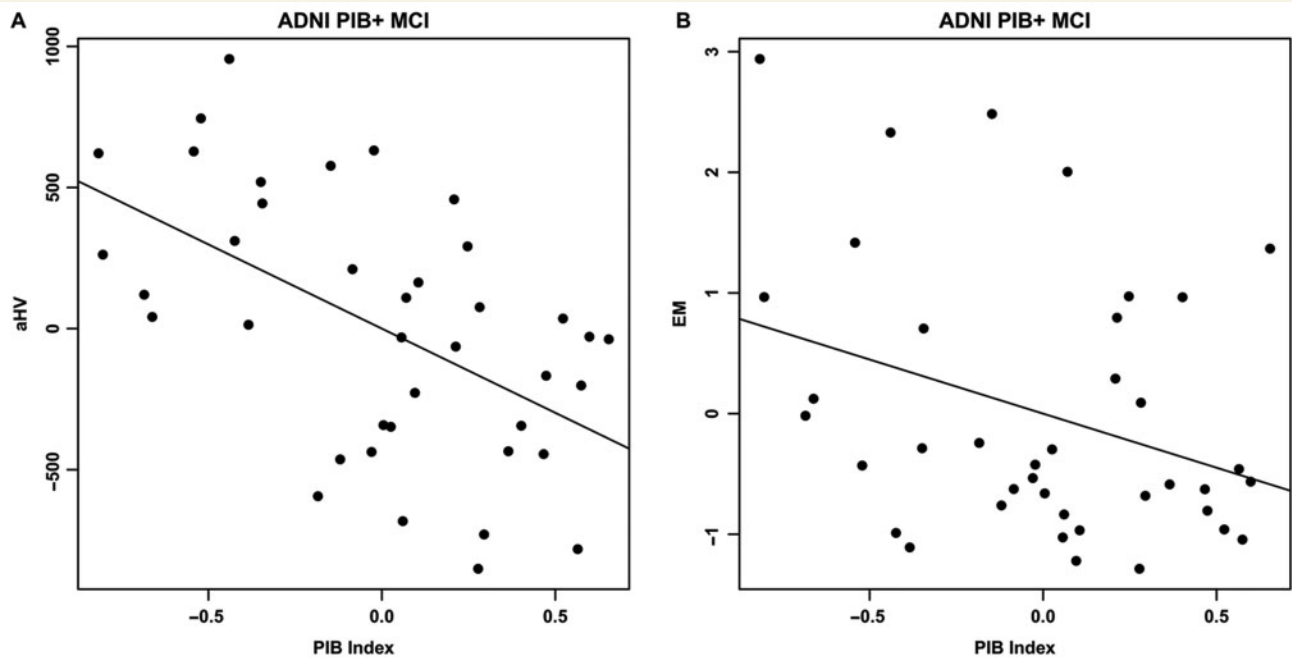


**Figure 7** Partial regression plots showing the relationships between PIB index and aHV (A) and EM (B) within the ADNI PIB+ MCI group. Residuals are plotted for each variable to adjust for the effects of age, gender and education. PIB index is significantly associated with both aHV and EM (A:  $\Delta R^2 = 0.27$ ,  $P = 0.00070$ ; B:  $\Delta R^2 = 0.11$ ,  $P = 0.046$ ).

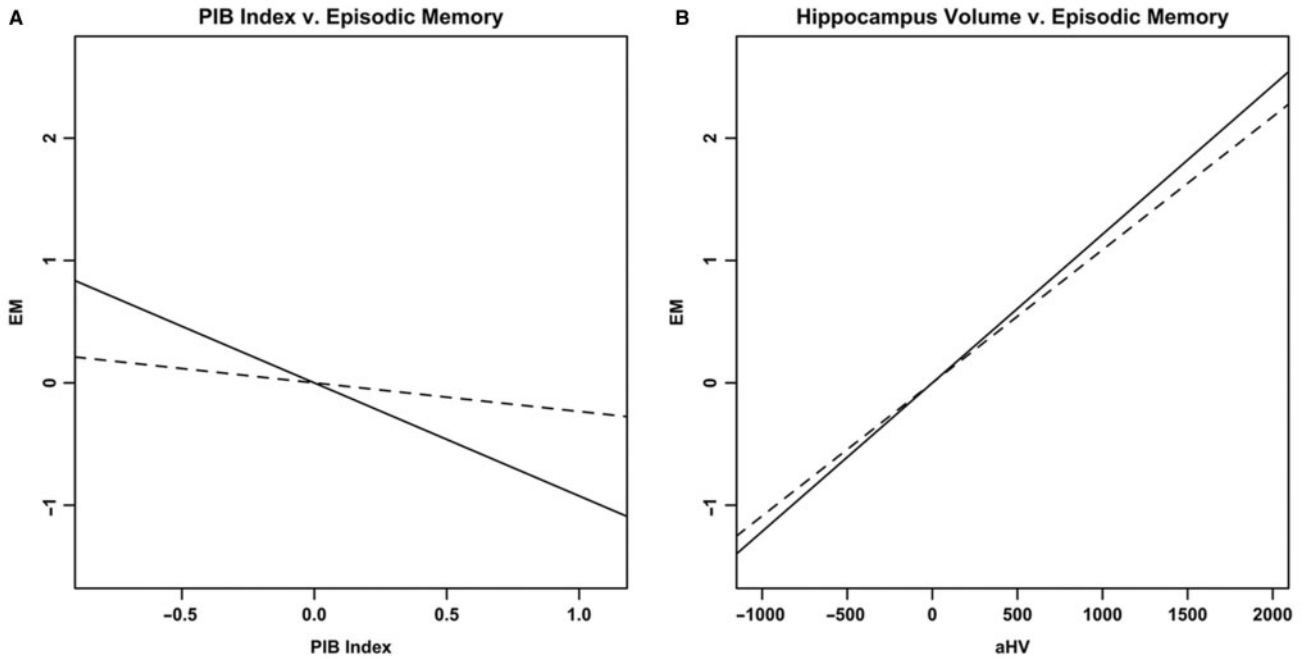


**Figure 8** Partial regression plots showing results from a recursive regression procedure suggesting a sequential relationship between the three variables, with aHV mediating the relationship between PIB index and EM. Residuals are plotted for each variable to adjust for the effects of age, gender and education. (A) The relationship between PIB index and EM before (solid line,  $P = 0.0044$ ) and after controlling for aHV (dashed line;  $\Delta R^2 = 0.00$ ,  $P = 0.50$ ). (B) The relationship between aHV and EM before (solid line,  $P = 0.000023$ ) and after controlling for PIB index (dashed line;  $\Delta R^2 = 0.15$ ,  $P = 0.0015$ ).

this pathology would help illuminate the role of NFTs in non-demented populations. A further possibility is that global A $\beta$  plaque quantities may be a marker of soluble A $\beta$  levels, which are undetected with PIB-PET imaging (Lockhart *et al.*, 2007). Soluble species are considered the most toxic form of A $\beta$ , and have been shown to correlate with synapse loss and disease severity better than A $\beta$  plaques (Walsh and Selkoe, 2007). Thus, soluble A $\beta$  may directly inflict hippocampal damage as plaques are deposited in cortex. Although the data presented in this study do not clarify the mechanism by which cortical A $\beta$  burden and HV atrophy are related, the reproducibility of this relationship across three samples gives convincing evidence that such a relationship exists.

## A $\beta$ burden and EM

We found a significant negative relationship between A $\beta$  burden and EM in our primary NC group, albeit driven by two high PIB subjects. This correlation was not replicated in the other cognitive domains examined (working memory and frontal function), suggesting that EM shows heightened vulnerability to A $\beta$  accumulation (at least when levels of this pathology are high). This finding is consistent with longitudinal data showing that in most subjects EM is the first cognitive domain compromised in the years leading to Alzheimer's disease onset (Small *et al.*, 2000; Grober *et al.*, 2008). One study to date has found a relationship between EM and PIB uptake within a group of normal individuals (Pike *et al.*, 2007), and it is possible that our study lacked the statistical power to replicate this finding after excluding the two highest PIB subjects.

Although modest PIB increases were associated with HV atrophy in our data, these increases were not accompanied by EM memory deficits after removal of the two subjects with highest PIB values. This dissociation between A $\beta$  burden and EM in this study may reflect a window in which cognitive reserve processes are sufficient to mask underlying pathological processes and brain atrophy (Stern, 2006). Supporting this hypothesis, it was recently shown that despite equivalent cognitive status, Alzheimer's disease subjects with high education show more PIB uptake than Alzheimer's disease subjects with low education (Kemppainen *et al.*, 2008). In addition, relationships between EM and PIB uptake were more pronounced in the MCI subjects in whom A $\beta$  levels are higher and reserve or compensatory processes are more likely to be exhausted. The role of cognitive reserve in dampening the relationship between A $\beta$  burden and cognitive deficits is speculative in this dataset, and future studies that examine whether cognitive reserve measures are a modifying factor are needed to address this possibility.

The lack of association between A $\beta$  burden and EM within the NC groups may also be explained by a sequential relationship between the three variables examined, with HV mediating the relationship between A $\beta$  burden and EM. In this study, we found evidence for this sequential relationship using a recursive regression procedure. A similar sequence has been suggested based on post-mortem findings demonstrating that NFTs mediate the relationship between A $\beta$  plaques and cognitive function (Bennett *et al.*, 2004). Our results mirror these findings, using imaging measures (PIB-PET and MRI-derived HV) as a surrogate for A $\beta$  and NFT pathologies. An indirect relationship between A $\beta$  burden and cognitive change would make an association between these measures difficult to detect (especially within small groups of non-demented subjects) and may explain discrepancies among the studies that have examined this relationship.

## Quantifying and classifying PIB uptake

We choose to quantify A $\beta$  burden by averaging values across multiple cortical areas, an approach that has been employed by many other groups (Fagan *et al.*, 2006; Mintun *et al.*, 2006; Pike *et al.*, 2007; Rowe *et al.*, 2007; Fotenos *et al.*, 2008; Jack *et al.*, 2008b). It has long been established that the pattern of A $\beta$  deposition varies between subjects (Braak and Braak, 1991) and we believe that this method gauges total A $\beta$  quantity without overemphasizing a single brain region. However, it is possible that regional deposition of A $\beta$  is biologically meaningful (Meyer-Luehmann *et al.*, 2008) and should be addressed in future PIB studies of aging.

The general trend amongst post-mortem and PIB-PET studies is to divide normal subjects into low- and high-pathology groups (Hulette *et al.*, 1998; Schmitt *et al.*, 2000; Goldman *et al.*, 2001; Jack *et al.*, 2002; Bennett *et al.*, 2006; Mintun *et al.*, 2006; Rowe *et al.*, 2007; Fotenos *et al.*, 2008). This approach is especially intriguing from the clinical perspective since it provides a possible diagnostic criterion for at-risk individuals. However, the cutoff point for determining low- and high-groups is somewhat arbitrary and ignores all accumulation below the determined threshold. Furthermore, our study agrees with previous PIB-PET studies in demonstrating that PIB uptake values are continuous rather than dichotomous in cognitively normal populations (Pike *et al.*, 2007; Rowe *et al.*, 2007; Jack *et al.*, 2008b). By treating PIB index as a continuous variable in our statistical models, we found that quantities below this 'high-level' cutoff are meaningful and coincide with hippocampal atrophy in normal elderly subjects. It is likely that the negative impact of A $\beta$  pathology begins during

**Table 2** Regression model summary

Regression Model	BAC NC, <i>n</i> = 20	BAC NC, <i>n</i> = 18	ADNI NC	ADNI PIB+ MCI
aHV = PIB	$\Delta R^2 = 0.45$ , <i>P</i> = 0.0016	$\Delta R^2 = 0.28$ , <i>P</i> = 0.026	$\Delta R^2 = 0.22$ , <i>P</i> = 0.047	$\Delta R^2 = 0.27$ , <i>P</i> = 0.00070
EM = PIB	$\Delta R^2 = 0.35$ , <i>P</i> = 0.0086	$\Delta R^2 = 0.03$ , <i>P</i> = 0.47	$\Delta R^2 = 0.02$ , <i>P</i> = 0.60	$\Delta R^2 = 0.11$ , <i>P</i> = 0.046

Regression models were conducted twice within the BAC NC group. The first analysis used the entire BAC NC sample (*n* = 20) whereas the second analysis was conducted after removing the two subjects with the highest PIB index (*n* = 18). Significant models are in bold. A consistent relationship between aHV and PIB index is observed in each group examined.

initial stages of accumulation in non-demented individuals, far before Alzheimer's disease-comparable levels are reached.

Classification of MCI subjects as PIB+ is motivated by research showing that MCI subjects with high PIB uptake are likely to convert to Alzheimer's disease (Forsberg *et al.*, 2008). Furthermore, a post-mortem study revealed that although the majority of amnesic MCI subjects that later convert to dementia have Alzheimer's disease pathology, 29% show pathology in the medial temporal lobe unrelated to Alzheimer's disease (Jicha *et al.*, 2006). Using an ROC-curve approach to dichotomize ADNI MCI subjects based on PIB index values, 75% were classified as PIB+ while 25% were classified as PIB-. These percentages are consistent with the aforementioned post-mortem study, and it is possible that pathological processes unrelated to Alzheimer's disease are present in the hippocampus of the PIB- MCI subjects. Since the focus of this study was to examine the relationships between A $\beta$  burden and preclinical Alzheimer's disease markers, we deemed regression analyses within the group of PIB+ MCI subjects to be the most appropriate. Follow-up to determine whether PIB+ MCI subjects convert to Alzheimer's disease and PIB- MCI subjects convert to other forms of dementia (such as Vascular Dementia, Frontotemporal Dementia, etc.) will provide further support for dichotomizing this group.

## Limitations

A main limitation in the present study is the small sample size of our NC group. We addressed this concern by removing outliers and using a replication group from ADNI. Furthermore, many differences exist between the primary and replication groups that may have confounded results (such as differences in demographics, imaging acquisition and neuropsychological testing). As larger samples are collected it will be possible to employ the replication group approach within a single cohort, achieving similarity across measures while varying the subjects in the primary and replication groups. Nevertheless, the reproducibility of results despite these differences suggests that the relationship between A $\beta$  burden and HV will generalize to other populations. However, subjects recruited through BAC and ADNI may not be representative of the general population (for example, both groups were highly educated). Additionally, the cross-sectional design of this study allows only speculation that elevated PIB index is a preclinical Alzheimer's disease marker. Longitudinal studies will help determine whether the presence of A $\beta$  plaques predicts Alzheimer's disease conversion, and whether this pathology precedes hippocampal atrophy and EM decline.

## Conclusions

Despite many differences across cohorts, we found an inverse relationship between A $\beta$  burden and HV in two independent samples of normal elderly subjects. This finding was also observed in a PIB+ MCI group, strengthening the implication that levels of PIB uptake in non-demented populations is biologically meaningful. The exact mechanisms underlying this relationship between cortical A $\beta$  burden and HV atrophy are unclear, and may reflect

disruption of cortico-hippocampal connectivity, co-occurrence of cortical A $\beta$  plaques and hippocampus NFTs, or the local impact of soluble A $\beta$  species in the hippocampus. Within our primary NC group, the relationship between A $\beta$  burden and EM was highly influenced by two high PIB subjects and did not replicate across different cohorts, suggesting that this relationship is more complex and may be modified by other factors (such as cognitive reserve and the degree of HV atrophy). The observed lack of association between A $\beta$  burden and EM may also reflect a sequential relationship between the examined variables, with HV atrophy mediating the relationship between A $\beta$  pathology and EM decline. Overall, these results suggest that low levels of A $\beta$  accumulation may reflect early Alzheimer's disease development and contribute to the HV atrophy and EM decline observed in studies of aging.

## Funding

National Institutes of Health (AG027859); and by the Alzheimer's Disease Neuroimaging Initiative (AG024904).

## References

- Aizenstein HJ, Nebes RD, Saxton JA, Price JC, Mathis CA, Tsopelas ND, et al. Amyloid deposition is frequent and often is not associated with significant cognitive impairment in the elderly. *Arch Neurol* 2008; 65: 1509–17.
- Apostolova LG, Dutton RA, Dinov ID, Hayashi KM, Toga AW, Cummings JL, et al. Conversion of mild cognitive impairment to Alzheimer disease predicted by hippocampal atrophy maps. *Arch Neurol* 2006; 63: 693–9.
- Arnold SE, Hyman BT, Flory J, Damasio AR, Van Hoesen GW. The topographical and neuroanatomical distribution of neurofibrillary tangles and neuritic plaques in the cerebral cortex of patients with Alzheimer's disease. *Cereb Cortex* 1991; 1: 103–16.
- Baron RM, Kenny DA. The moderator-mediator variable distinction in social psychological research: conceptual, strategic, and statistical considerations. *J Pers Soc Psychol* 1986; 51: 1173–82.
- Bennett DA, Schneider JA, Arvanitakis Z, Kelly JF, Aggarwal NT, Shah RC, et al. Neuropathology of older persons without cognitive impairment from two community-based studies. *Neurology* 2006; 66: 1837–44.
- Bennett DA, Schneider JA, Wilson RS, Bienias JL, Arnold SE. Neurofibrillary tangles mediate the association of amyloid load with clinical Alzheimer disease and level of cognitive function. *Arch Neurol* 2004; 61: 378–84.
- Braak H, Braak E. Neuropathological staging of Alzheimer-related changes. *Acta Neuropathol* 1991; 82: 239–59.
- Braak H, Braak E. Frequency of stages of Alzheimer-related lesions in different age categories. *Neurobiol Aging* 1997; 18: 351–7.
- Buckner RL, Head D, Parker J, Fotenos AF, Marcus D, Morris JC, et al. A unified approach for morphometric and functional data analysis in young, old, and demented adults using automated atlas-based head size normalization: reliability and validation against manual measurement of total intracranial volume. *Neuroimage* 2004; 23: 724–38.
- Dale AM, Fischl B, Sereno MI. Cortical surface-based analysis. I. Segmentation and surface reconstruction. *Neuroimage* 1999; 9: 179–94.
- Davis DG, Schmitt FA, Wekstein DR, Markesbery WR. Alzheimer neuropathologic alterations in aged cognitively normal subjects. *J Neuropathol Exp Neurol* 1999; 58: 376–88.
- de Leon MJ, Convit A, George AE, Golomb J, de Santi S, Tarshish C, et al. In vivo structural studies of the hippocampus in normal aging

- and in incipient Alzheimer's disease. *Ann N Y Acad Sci* 1996; 777: 1–13.
- Delis D, Kramer J, Kaplan E, Ober B. California verbal learning test. San Antonio: The Psychological Corporation; 2000.
- Desikan RS, Segonne F, Fischl B, Quinn BT, Dickerson BC, Blacker D, et al. An automated labeling system for subdividing the human cerebral cortex on MRI scans into gyral based regions of interest. *Neuroimage* 2006; 31: 968–80.
- Fagan AM, Mintun MA, Mach RH, Lee SY, Dence CS, Shah AR, et al. Inverse relation between in vivo amyloid imaging load and cerebrospinal fluid Abeta42 in humans. *Ann Neurol* 2006; 59: 512–9.
- Fischl B, Liu A, Dale AM. Automated manifold surgery: constructing geometrically accurate and topologically correct models of the human cerebral cortex. *IEEE Trans Med Imaging* 2001; 20: 70–80.
- Fischl B, Salat DH, Busa E, Albert M, Dieterich M, Haselgrove C, et al. Whole brain segmentation: automated labeling of neuroanatomical structures in the human brain. *Neuron* 2002; 33: 341–55.
- Forsberg A, Engler H, Almkvist O, Blomqvist G, Hagman G, Wall A, et al. PET imaging of amyloid deposition in patients with mild cognitive impairment. *Neurobiol Aging* 2008; 29: 1456–65.
- Fotenus AF, Mintun MA, Snyder AZ, Morris JC, Buckner RL. Brain volume decline in aging: evidence for a relation between socioeconomic status, preclinical Alzheimer disease, and reserve. *Arch Neurol* 2008; 65: 113–20.
- Goldman WP, Price JL, Storandt M, Grant EA, McKeel DW Jr, Rubin EH, et al. Absence of cognitive impairment or decline in preclinical Alzheimer's disease. *Neurology* 2001; 56: 361–7.
- Greicius MD, Srivastava G, Reiss AL, Menon V. Default-mode network activity distinguishes Alzheimer's disease from healthy aging: evidence from functional MRI. *Proc Natl Acad Sci USA* 2004; 101: 4637–42.
- Grober E, Hall CB, Lipton RB, Zonderman AB, Resnick SM, Kawas C. Memory impairment, executive dysfunction, and intellectual decline in preclinical Alzheimer's disease. *J Int Neuropsychol Soc* 2008; 14: 266–78.
- Hardy J, Selkoe DJ. The amyloid hypothesis of Alzheimer's disease: progress and problems on the road to therapeutics. *Science* 2002; 297: 353–6.
- Hulette CM, Welsh-Bohmer KA, Murray MG, Saunders AM, Mash DC, McIntyre LM. Neuropathological and neuropsychological changes in 'normal' aging: evidence for preclinical Alzheimer disease in cognitively normal individuals. *J Neuropathol Exp Neurol* 1998; 57: 1168–74.
- Jack CR Jr, Bernstein MA, Fox NC, Thompson P, Alexander G, Harvey D, et al. The Alzheimer's disease neuroimaging initiative (ADNI): MRI methods. *J Magn Reson Imaging* 2008a; 27: 685–91.
- Jack CR Jr, Dickson DW, Parisi JE, Xu YC, Cha RH, O'Brien PC, et al. Antemortem MRI findings correlate with hippocampal neuropathology in typical aging and dementia. *Neurology* 2002; 58: 750–7.
- Jack CR Jr, Lowe VJ, Senjem ML, Weigand SD, Kemp BJ, Shiung MM, et al. 11C PiB and structural MRI provide complementary information in imaging of Alzheimer's disease and amnesic mild cognitive impairment. *Brain* 2008b; 131: 665–80.
- Jack CR Jr, Petersen RC, Xu YC, O'Brien PC, Smith GE, Ivnik RJ, et al. Prediction of AD with MRI-based hippocampal volume in mild cognitive impairment. *Neurology* 1999; 52: 1397–403.
- Jicha GA, Parisi JE, Dickson DW, Johnson K, Cha R, Ivnik RJ, et al. Neuropathologic outcome of mild cognitive impairment following progression to clinical dementia. *Arch Neurol* 2006; 63: 674–81.
- Katzman R, Terry R, DeTeresa R, Brown T, Davies P, Fuld P, et al. Clinical, pathological, and neurochemical changes in dementia: a subgroup with preserved mental status and numerous neocortical plaques. *Ann Neurol* 1988; 23: 138–44.
- Kemppainen NM, Aalto S, Karrasch M, Nagren K, Savisto N, Oikonen V, et al. Cognitive reserve hypothesis: Pittsburgh Compound B and fluorodeoxyglucose positron emission tomography in relation to education in mild Alzheimer's disease. *Ann Neurol* 2008; 63: 112–8.
- Kemppainen NM, Aalto S, Wilson IA, Nagren K, Helin S, Bruck A, et al. Voxel-based analysis of PET amyloid ligand [11C]PiB uptake in Alzheimer disease. *Neurology* 2006; 67: 1575–80.
- Klunk WE, Engler H, Nordberg A, Wang Y, Blomqvist G, Holt DP, et al. Imaging brain amyloid in Alzheimer's disease with Pittsburgh Compound-B. *Ann Neurol* 2004; 55: 306–19.
- Knopman DS, Parisi JE, Salviati A, Floriach-Robert M, Boeve BF, Ivnik RJ, et al. Neuropathology of cognitively normal elderly. *J Neuropathol Exp Neurol* 2003; 62: 1087–95.
- Kramer JH, Jurik J, Sha SJ, Rankin KP, Rosen HJ, Johnson JK, et al. Distinctive neuropsychological patterns in frontotemporal dementia, semantic dementia, and Alzheimer disease. *Cogn Behav Neurol* 2003; 16: 211–8.
- Langstrom B, Antoni G, Gullberg P, Halldin C, Malmberg P, Nagren K, et al. Synthesis of L- and D-[methyl-11C]methionine. *J Nucl Med* 1987; 28: 1037–40.
- Link JM, Krohn KA, Clark JC. Production of [11C]CH3I by single pass reaction of [11C]CH4 with I2. *Nucl Med Biol* 1997; 24: 93–7.
- Lockhart A, Lamb JR, Osredkar T, Sue LI, Joyce JN, Ye L, et al. PIB is a non-specific imaging marker of amyloid-beta (Abeta) peptide-related cerebral amyloidosis. *Brain* 2007; 130: 2607–15.
- Logan J, Fowler JS, Volkow ND, Wang GJ, Ding YS, Alexoff DL. Distribution volume ratios without blood sampling from graphical analysis of PET data. *J Cereb Blood Flow Metab* 1996; 16: 834–40.
- Mathalon DH, Sullivan EV, Rawles JM, Pfefferbaum A. Correction for head size in brain-imaging measurements. *Psychiatry Res* 1993; 50: 121–39.
- Mathis CA, Wang Y, Holt DP, Huang GF, Debnath ML, Klunk WE. Synthesis and evaluation of 11C-labeled 6-substituted 2-arylbenzothiazoles as amyloid imaging agents. *J Med Chem* 2003; 46: 2740–54.
- McKhann G, Drachman D, Folstein M, Katzman R, Price D, Stadlan EM. Clinical diagnosis of Alzheimer's disease: report of the NINCDS-ADRDA Work Group under the auspices of Department of Health and Human Services Task Force on Alzheimer's Disease. *Neurology* 1984; 34: 939–44.
- Meltzer CC, Kinahan PE, Greer PJ, Nichols TE, Comtat C, Cantwell MN, et al. Comparative evaluation of MR-based partial-volume correction schemes for PET. *J Nucl Med* 1999; 40: 2053–65.
- Meyer-Luehmann M, Spires-Jones TL, Prada C, Garcia-Alloza M, de Calignon A, Rozkalne A, et al. Rapid appearance and local toxicity of amyloid-beta plaques in a mouse model of Alzheimer's disease. *Nature* 2008; 451: 720–4.
- Mintun MA, Larossa GN, Sheline YI, Dence CS, Lee SY, Mach RH, et al. [11C]PiB in a nondemented population: potential antecedent marker of Alzheimer disease. *Neurology* 2006; 67: 446–52.
- Morris JC. The clinical dementia rating (CDR): current version and scoring rules. *Neurology* 1993; 43: 2412–4.
- Pike KE, Savage G, Villemagne VL, Ng S, Moss SA, Maruff P, et al. Beta-amyloid imaging and memory in non-demented individuals: evidence for preclinical Alzheimer's disease. *Brain* 2007; 130: 2837–44.
- Price JC, Klunk WE, Lopresti BJ, Lu X, Hoge JA, Ziolk SK, et al. Kinetic modeling of amyloid binding in humans using PET imaging and Pittsburgh Compound-B. *J Cereb Blood Flow Metab* 2005; 25: 1528–47.
- Price JL, Morris JC. Tangles and plaques in nondemented aging and 'preclinical' Alzheimer's disease. *Ann Neurol* 1999; 45: 358–68.
- Ranganath C, Heller A, Cohen MX, Brozinsky CJ, Rissman J. Functional connectivity with the hippocampus during successful memory formation. *Hippocampus* 2005; 15: 997–1005.
- Raz N, Rodrigue KM. Differential aging of the brain: patterns, cognitive correlates and modifiers. *Neurosci Biobehav Rev* 2006; 30: 730–48.
- Reitan RM. Validity of the trailmaking test as an indication of organic brain damage. *Percept Mot Skills* 1958; 8: 271–6.
- Rowe CC, Ng S, Ackermann U, Gong SJ, Pike K, Savage G, et al. Imaging beta-amyloid burden in aging and dementia. *Neurology* 2007; 68: 1718–25.
- Salthouse TA, Babcock RL, Shaw RJ. Effects of adult age on structural and operational capacities in working memory. *Psychol Aging* 1991; 6: 118–27.

- Schmitt FA, Davis DG, Wekstein DR, Smith CD, Ashford JW, Markesbery WR. 'Preclinical' AD revisited: neuropathology of cognitively normal older adults. *Neurology* 2000; 55: 370–6.
- Segonne F, Dale AM, Busa E, Glessner M, Salat D, Hahn HK, et al. A hybrid approach to the skull stripping problem in MRI. *Neuroimage* 2004; 22: 1060–75.
- Small BJ, Fratiglioni L, Viitanen M, Winblad B, Backman L. The course of cognitive impairment in preclinical Alzheimer disease: three- and 6-year follow-up of a population-based sample. *Arch Neurol* 2000; 57: 839–44.
- Small SA, Stern Y, Tang M, Mayeux R. Selective decline in memory function among healthy elderly. *Neurology* 1999; 52: 1392–6.
- Smith CD, Chebrolu H, Wekstein DR, Schmitt FA, Jicha GA, Cooper G, et al. Brain structural alterations before mild cognitive impairment. *Neurology* 2007; 68: 1268–73.
- Stern Y. Cognitive reserve and Alzheimer disease. *Alzheimer Dis Assoc Disord* 2006; 20: S69–S74.
- Tomlinson BE, Blessed G, Roth M. Observations on the brains of non-demented old people. *J Neurol Sci* 1968; 7: 331–56.
- Villemagne VL, Pike KE, Darby D, Maruff P, Savage G, Ng S, et al. Abeta deposits in older non-demented individuals with cognitive decline are indicative of preclinical Alzheimer's disease. *Neuropsychologia* 2008; 46: 1688–97.
- Walsh DM, Selkoe DJ. A beta oligomers—a decade of discovery. *J Neurochem* 2007; 101: 1172–84.
- Wang L, Zang Y, He Y, Liang M, Zhang X, Tian L, et al. Changes in hippocampal connectivity in the early stages of Alzheimer's disease: evidence from resting state fMRI. *Neuroimage* 2006; 31: 496–504.
- Wechsler D. Wechsler adult intelligence scale-revised. San Antonio: The Psychological Corporation; 1987a.
- Wechsler D. Wechsler memory scale-revised. San Antonio: The Psychological Corporation; 1987b.
- Wilson AA, Garcia A, Chestakova A, Kung H, Houle S. A rapid one-step radiosynthesis of the beta-amyloid imaging radiotracer N-methyl-<sup>11</sup>C-2-(4'-methylaminophenyl)-6-hydroxybenzothiazole (<sup>11</sup>C]-6-OH-BTA-1). *J Labelled Compounds and Radiopharmaceuticals* 2004; 47: 679–82.
- Zaidi H, Ruest T, Schoenahl F, Montandon ML. Comparative assessment of statistical brain MR image segmentation algorithms and their impact on partial volume correction in PET. *Neuroimage* 2006; 32: 1591–607.
- Zec RF. The stroop color-word test: A paradigm for procedural learning. *Arch Clin Neuropsychol* 1986; 1: 274–5.